Reaction Mechanisms and Kinetics for the Oxidations of Dimethyl Sulfide, Dimethyl Disulfide, and Methyl Mercaptan by the Nitrate Radical

Justin Jee and Fu-Ming Tao*

Department of Chemistry and Biochemistry, California State University, Fullerton, California 92834

Received: November 17, 2005; In Final Form: April 25, 2006

This study examines the initial oxidation routes of the three major reduced sulfur compounds (CH_3SH, CH_3SCH_3, and CH_3SSCH_3) by the nitrate radical using density functional and ab initio methods. Stationary points along each reaction pathway are examined using different levels of theory and basis sets to ensure the convergence of the results. Kinetics calculations follow on the determined reaction pathways to obtain the rate constants. This study shows that sulfur compounds exhibit a general trend of hydrogen abstraction following the formation of an initial sulfur-nitrate complex. The results are in agreement with experimental work on CH_3SCH_3 and CH_3SH, while refuting a proposal of several previous studies that oxygen addition is the dominant oxidation pathway in the case of CH_3SSCH_3. The rate constants obtained from kinetics calculations are consistent with experimental findings and exhibit negative temperature dependence. Overall, this study confirms the importance of nitrate in the oxidation of reduced sulfur compounds in the atmosphere.

Introduction

Methyl mercaptan (CH_3SH), dimethyl sulfide (DMS; CH_3SCH_3), and dimethyl disulfide (DMDS; CH_3SSCH_3) are the most abundant reduced sulfur compounds in the atmosphere as well as the dominant sulfur species in the troposphere released by biogenic sources. DMS alone, released by plankton into the marine boundary layer, comprises over 25% of the world's sulfur budget, and methyl mercaptan and DMDS both contribute 3−10% of the sulfur flux above land.[1] Because these compounds are highly reactive in the gas phase, ultimately leading to sulfate, their decomposition has been studied extensively in experimental and field studies.[2]

Although reduced sulfur compounds are most commonly oxidized by the hydroxyl radical (OH) during the day, their reaction with the nitrate radical (NO_3) is predominant at night and in areas of high nitrate concentration. An early experimental study by Atkinson et al.[3] demonstrated that the DMS + NO_3 rate constant is 5.4×10^{-13} cm^3 molecule^{-1} s^{-1}, fast enough to imply that nitrate is the main source of DMS oxidation in areas of high nitrate concentrations. These results are in agreement with the flash-photolysis experiments performed by Wallington et al.,[4] who predicted a rate of 8.3×10^{-13} cm^3 molecule^{-1} s^{-1} for the DMS + NO_3 reaction with negative temperature dependence. Jensen et al.[5] confirmed that the reaction mechanism for this reaction was hydrogen abstraction leading to nitric acid and the CH_3SH_2 radical, which later decomposed into sulfur dioxide and methanesulfonic acid. Tyndall et al.[6] noted a faster rate constant of 1.0×10^{-12} cm^3 molecule^{-1} s^{-1} independent of temperature in the range 278−318 K. Later, fast flow reactor experiments with LIF detection of NO_3 performed by Dlugokencky and Howard[7] predicted a slightly slower rate constant for DMS + NO_3 but a slightly faster rate constant for methyl mercaptan's reaction with nitrate radical of 1.09×10^{-12} cm^3 molecule^{-1} s^{-1}. This study also predicted a moderate rate constant for DMDS and nitrate radical of 5.4×10^{-13} cm^3 molecule^{-1} s^{-1}. From these studies it is clear that the oxidation of reduced sulfur compounds, particularly through oxidation by free radicals, has enormous atmospheric implications because it accounts for a significant amount of atmospheric sulfuric acid and sulfate aerosols, major components of cloud condensation nuclei and acid rain.[1,2] Furthermore, the kinetics of the reactions is clearly favorable in the troposphere. Details regarding the mechanisms of these oxidations are, however, still elusive.

Winer et al.[8] first demonstrated nitrate's potential as an oxidizing agent in the troposphere using computer simulations based on kinetic and ambient concentration data. More recently, field studies over Antarctic water by Toole et al.[9] and off the coast of Crete by Bardouki et al.[10] have shown that ambient nitrate concentrations can control the diurnal flux of DMS oxidation, especially in polluted areas. Because of such reasons, an understanding of nitrate's role as an initial oxidizing agent of reduced sulfur compounds is crucial in achieving a complete picture of the atmospheric sulfur cycle. Finally, a study of the oxidation of these reduced sulfur compounds by the nitrate is important as their interaction represents a direct connection between the nitrogen and sulfur cycles in the atmosphere.[11]

The oxidations of DMS and methyl mercaptan by nitrate radical are believed to follow a hydrogen abstraction pathway whereas the oxidation of DMDS by nitrate radical is believed to follow an oxygen addition pathway producing nitrite, CH_3S, and CH_3SO.[12] However, in this study we consider both hydrogen abstraction and oxygen addition for DMDS oxidation to ensure that all possibilities are accounted for. The four reactions considered are as follows:

$$CH_3SCH_3 + NO_3 \rightarrow CH_3S(ONO_2)CH_3 \rightarrow CH_3SCH_2 + HNO_3 \quad (1)$$

$$CH_3SH + NO_3 \rightarrow CH_3S(ONO_2)H \rightarrow CH_3S + HNO_3 \quad (2)$$

* To whom the correspondence should be addressed. E-mail: ftao@fullerton.edu.

10.1021/jp0566717 CCC: $33.50
Published on Web 05/26/2006

$$CH_3SSCH_3 + NO_3 \rightarrow CH_3SS(ONO_2)CH_3 \rightarrow CH_3SSOCH_3 + NO_2 \quad (3)$$

$$CH_3SSCH_3 + NO_3 \rightarrow CH_3SS(ONO_2)CH_3 \rightarrow CH_3SSCH_2 + HNO_3 \quad (4)$$

Note that in the case of reaction 3, CH_3SSOCH_3 is predicted to decompose into CH_3S and CH_3SO. Daykin and Wine[13] studied the pressure dependence of reaction 1 using a laser flash photolysis-long path laser absorption technique, with no dependence observed. Jensen et al.[12] performed chamber experiments on the nitrate reaction with all three reduced sulfur compounds. In all three cases, methanesulfonic acid (CH_3SO_3H), sulfur dioxide (SO_2), formaldehyde (CH_2O), methyl nitrate (CH_3ONO_2), nitric acid (HNO_3), and CH_3SNO_2 were found as final products. A peroxynitrate compound was discovered for a short period of time after nitrate was mixed with DMS and methyl mercaptan. Thus those reactions are believed to proceed via the formation of an adduct complex, followed by hydrogen abstraction.

DMDS is not as common as DMS or methyl mercaptan; however, it is abundant enough in the atmosphere and reactive enough to be considered an important source of sulfuric acid and sulfate aerosols, as demonstrated in a field study near Antarctica by Jefferson et al.[14] Unfortunately, the reaction of DMDS with nitrate is complex. Although Jensen et al.[12] found a peroxynitrate compound after DMDS and nitrate were mixed, the peroxynitrate's spectral features were much weaker than those found in the DMS and methyl mercaptan reactions. However, the products formed from the complete decomposition of DMDS are the same as those produced by decomposition of DMS and methyl mercaptan. According to Jensen et al.,[12] it would seem that CH_3S and CH_3SO radicals are intermediates in the decomposition of DMDSO because they are intermediates in DMS and methyl mercaptan decomposition. Thus Jensen et al.[12] proposed that the mechanism for oxidation of DMDS by nitrate must be addition of oxygen to a sulfur atom followed by decomposition to CH_3S, CH_3SO, and NO_2.

This proposed mechanism appears to explain products formed. However, it fails to explain discrepancies in their quantification. For example, if DMDS followed the decomposition pathway suggested by Jensen et al.,[12] it should produce about twice as much formaldehyde as methyl mercaptan does. In fact, DMDS produces three times as much formaldehyde as methyl mercaptan does according to their chamber experiment. Also, there is a large percent error reported for the percent yield of sulfur dioxide and methanesulfonic acid: a range of up to 20%. For such reasons, it appears that there is some aspect of DMDS decomposition that is not well understood. Thus, this study considers more than one pathway for DMDS oxidation by the nitrate radical. Determination of which pathway is more likely—oxygen addition or hydrogen abstraction—is vital to an understanding of DMDS decomposition in the troposphere.

Tyndall and Ravishankara[2] conducted a study on the reaction kinetics of organic sulfides with the nitrate radical that reviewed rate constants from several of the experiments listed above and provided suggested rate constants based on the average result of available experiments. The rate constant suggested by Tyndall and Ravishankara[2] for the DMS reaction with nitrate at 298 K and 1 atm is 1.0×10^{-12} cm^3 molecule^{-1} s^{-1}, and the rate constant for the methyl mercaptan reaction with nitrate under similar conditions is 0.9×10^{-12} cm^3 molecule^{-1} s^{-1}. These relatively fast rate constants indicate that their respective reactions are significant in the atmosphere. Experiments by Mac Leod et al.[15] give a rate constant of 0.4×10^{-13} cm^3 molecule^{-1} s^{-1} for the DMDS + NO_3 reaction, and Tyndall and Ravishankara[2] report that this reaction exhibits moderate negative temperature dependence in accordance with experiments by Wallington et al.[4] The temperature dependency of all three reactions will be discussed further in the results section.

This study uses theoretical calculations to provide details regarding the initial oxidation of DMS, DMDS, and methyl mercaptan by nitrate radical. The stationary points along each reaction pathway, including the separate reactants, reactant complex (RC), transition state, product complex (PC), and separate products, are fully characterized in terms of energy, geometry, frequency, and other molecular properties. The significance of nitrate−sulfur adduct complexes is evaluated according to the stability relative to separate reactants. The optimized transition state is employed to calculate the rate constants at different temperatures via kinetic theory. The calculated reaction pathways along with the rate constants confirm the experimentally suggested mechanisms of DMS and methyl mercaptan reactions. In the case of DMDS, however, hydrogen abstraction, instead of oxygen addition, is likely the preferred pathway for the oxidation of DMDS by nitrate, contrary to the route proposed by Jensen et al.[12]

Theoretical Methods

Quantum Chemical Calculations. Each reaction pathway considered is represented in terms of separate reactants, a reactant complex (RC), a transition state, a product complex (PC), and separate products. Initial geometries for these stationary states were chosen on the basis of favorable electrostatic interactions and hydrogen bonding between the reacting species. Alternative geometries for the reactant and product complexes were tested to ensure that the lowest energy reaction pathway is reported for a given system. Finally, the validity of our transition state was verified using IRC calculations. Using the optimized geometry of the transition state, we analyzed the minimum energy path of the reaction and found that it supported the results of our RC, transition state, and PC with respect to geometry and energy. Geometry optimizations, frequency calculations, and energy calculations were performed using theories and basis sets as implemented in the Gaussian 03 program.[16]

Density functional theory (DFT) and ab initio theory were used to characterize the reaction pathways of all four reactions. Three different DFT methods were used: Becke's three-parameter functional with gradient-corrected correlation of Lee, Yang, and Parr (B3LYP),[17] the Becke half and half-functional with similar corrections (BH&HLYP),[18] and the "new generation" meta hybrid theory, BB1K.[19] Although B3LYP is a popular method for studying complexes such as those considered in this work, studies[20,21] have shown that B3LYP systematically underestimates reaction barrier heights, particularly in hydrogen abstraction. BH&HLYP is known to produce relatively more accurate barrier heights than B3LYP.[20,21] Two Pople basis sets, 6-31+G(d) and 6-311++G(d,p), were used in these DFT calculations. The recently developed BB1K functional[19] is a meta hybrid DFT functional that was tested against a database of 42 reactions to achieve a Hartree−Fock/Becke 95 parameter hybrid exchange ratio favorable to the production of accurate rate constants. However, although work by Zhao et al.[19] has proven BB1K to be reliable for relatively small radicals such as hydroxyl, chlorine, and hydrogen, its usefulness with reactions involving larger nitrate radicals remains untested. BB1K calculations in this study were performed using the aug-cc-pVDZ basis set.

TABLE 1: Relative Energies, Enthalpies, and Free Energies (in kcal mol^{-1}, at 298 K and 1 atm) of the Reacting Systems with Respect to Separate Reactants Calculated from Various Theories[a]

	electronic energies				ZPE-corrected		enthalpies		free energies	
theory/basis set	ΔE_{RC}	$\Delta E^{\ddagger}$	ΔE_{PC}	ΔE	$\Delta E^{\ddagger}_{ZP}$	ΔE_{ZP}	$\Delta H^{\ddagger}$	ΔH	$\Delta G^{\ddagger}$	ΔG
Dimethyl Sulfide, Reaction 1										
B3LYP/6-311++G(d,p)	−14.96	−4.98	−12.40	−5.57	−5.34	−4.72	−5.92	−4.75	4.49	−5.71
MP2/6-311++G(d,p)	−1.96	11.24	−6.23	1.36	7.39	−2.35	7.01	−2.00	17.42	−3.50
MP2/aug-cc-pVDZ	−3.65	9.87	−7.23	4.65	5.83	−1.87	5.49	−1.50	15.67	−3.08
BH&HLYP/6-311++G(d,p)	−14.31	−1.80	−17.08	−10.42	−2.85	−10.82	−3.33	−10.59	8.26	−10.95
BB1K/aug-cc-pVDZ		−5.09		−11.28						
CCSD(T)/6-311++G(d,p)[b]		−0.13		−7.68						
Methyl Mercaptan, Reaction 2										
B3LYP/6-311++G(d,p)	−9.93	−7.73	−23.34	−16.49	−6.13	−13.38	−6.88	−13.82	3.55	−13.96
MP2/6-311++G(d,p)		3.82		−11.22	1.98	−12.81	1.44	−12.79	11.77	−13.71
MP2/aug-cc-pVDZ		1.35		−8.15	−0.37	−12.47	−0.91	−12.50	9.37	−13.33
BH&HLYP/6-311++G(d,p)	−9.26	−7.04	−30.33	−22.88	−6.38	−20.68	−6.95	−20.89	4.32	−20.38
BB1K/aug-cc-pVDZ		−10.16		−21.65						
CCSD(T)/6-311++G(d,p)[b]		−5.73		−18.80						
Dimethyl Disulfide (Hydrogen Abstraction), Reaction 3										
B3LYP/6-311++G(d,p)	−10.61	−0.31	−8.88	−4.03	−1.04	−3.17	−1.45	−3.30	7.66	−4.06
BH&HLYP/6-311++G(d,p)	−9.04	4.02	−13.61	−8.94	2.64	−9.26	2.48	−9.17	12.74	−9.28
BB1K/aug-cc-pVDZ		6.11		−9.58						
CCSD(T)/6-311++G(d,p)[c]		2.71		−6.96						
Dimethyl Disulfide (Oxygen Addition), Reaction 4										
B3LYP/6-311++G(d,p)	−10.61	12.53	−23.35	−21.30	14.06	−20.29	13.93	−20.30	23.93	−20.60
BH&HLYP/6-311++G(d,p)	−9.04	18.68	−25.11	−18.25	18.78	−22.06	18.82	−21.84	30.02	−21.34
BB1K/aug-cc-pVDZ		15.95		−23.70						
CCSD(T)/6-311++G(d,p)[c]		17.86		−25.44						

[a] ΔE_{RC} stands for energy of the reactant complex, $\Delta E^{\ddagger}$ for energy of the transition state complex, ΔE_{PC} for energy of the product complex, ΔE for the overall change in energy for the reaction; similar notations are for ZPE-corrected energy, enthalpy, and free energy. [b] Using MP2/6-311++g(d,p) geometries. [c] Using BH&HLYP/6-311++G(d,p) geometries.

Two ab initio methods were used and they were, respectively, Møller−Plesset perturbation theory (MP2)[22] and coupled cluster theory with corrections for single, double, and triple excitations CCSD(T).[23] Results from ab initio methods may potentially be very different from those of DFT methods; the consistency of results between the two major theories may be viewed as a strong indication for the reliability of results. The MP2 method tends to overestimate reaction barrier heights,[20,21] which is again reflected in this work. As a result, single point CCSD(T) calculations using optimized geometries from the other methods would achieve more accurate results on relative energies. For reactions 1 and 2, geometry optimizations were carried out at the MP2 level using the 6-31+G(d), 6-311++G(d,p), and aug-cc-pVDZ basis sets, followed by CCSD(T) calculations on the MP2/6-311++G(d,p) geometries. For reactions 3 and 4, geometry optimizations at the MP2 level using the 6-311++G(d,p) and aug-cc-pVDZ basis sets were omitted after preliminary results using the 6-31+G(d) basis set indicated that the geometries would be similar to those of BH&HLYP. CCSD(T) calculations were performed on all reaction pathways using the 6-311++G(d,p) basis set. Relative energies, enthalpies, and free energies along the reaction pathways, all with respect to the separate reactants, are shown in Table 1. Relative energies from BH&HLYP/6-311++G(d,p) calculations are also shown in Figure 1. The results of geometry optimizations are summarized in Figures 2−4. IRC calculations were performed on all pathways at the BH&HLYP/6-311++G(d,p) level and confirmed the energy pathways. The geometries obtained from these IRC calculations are consistent with those shown in Figures 2−4.

Kinetics Calculation. Kinetics calculations were performed using classical transition state theory with Eckart tunneling corrections for reactions with positive activation energy. The kinetics calculations, based on reaction pathways determined from the available B3LYP, BH&HLYP, BB1K, MP2, and CCSD(T) results, determine the rate constants, k, for all reaction pathways. Table 2 shows the rate constants at a range of 260−310 K at 10 K intervals corresponding to BH&HLYP/6-311++G(d,p) results. Note that the activation energy is defined as the difference in energy between the transition state and the separate reactants. The free energies of the reactions can be used to determine the equilibrium constants of the reactions. The kinetics calculations were performed using the online service provided at the University of Utah.[24] Because the reverse rate constants of these reactions were several orders of magnitude smaller than those of the forward rate constants, only forward rate constants are reported here. The results of these kinetics calculations, along with results of experiments in the range 260−310 K, are summarized in Table 2.

Results and Discussion

Dimethyl Sulfide. For the reaction of DMS with the nitrate radical, hydrogen abstraction leading to nitric acid and $CH_3SCH_2^{\bullet}$ is the most likely pathway. This assertion is made on the basis that all quantum chemical calculations using different methods and kinetics calculations consistently support this pathway, which is also supported by experiments.

The peroxynitrate compound discovered in chamber experiments[2,7] is explained by the relatively high strength of the reactant complex between the nitrate and sulfur atoms of DMS. In the DMS reactant complex, the bond distance between the sulfur atom and oxygen atom on the nitrate radical is relatively close: 2.27 Å (see Figure 2). Both B3LYP and BH&HLYP predict high dissociation energy of 10−15 kcal/mol for these nitrate−sulfur complexes (see Table 1). Thus, the experimental hypothesis that the first step in the reaction between nitrate and DMS is the formation of an adduct complex is supported by theory. This strong interaction is most likely due to the opposite charges of the sulfur and oxygen atoms in the system. The

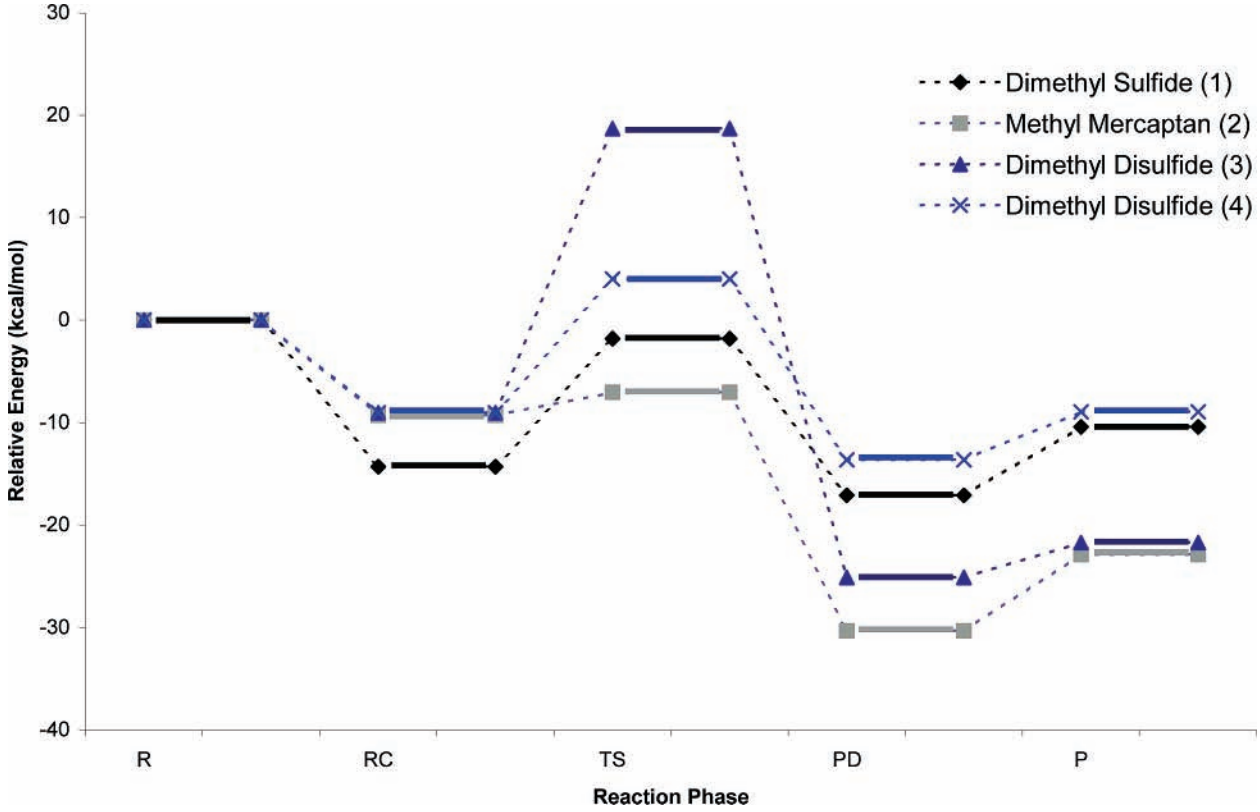

Figure 1. Relative energies of reacting systems along the reaction coordinate the separate reactants (R), reactant complex (RC), transition state (TS), product complex (PC), and separate products (P) for reactions 1−4). The energy values are from BH&HLYP/6-311++G(d,p) calculations.

TABLE 2: Rate Constants (in cm^3 $molecule^{-1}$ s^{-1}) Obtained from Transition State Theory for Reactions 1−4 at Different Temperatures (in K) Using BH&HLYP/6-311++G(d,p) and CCSD(T)/6-311++G(d,p)[a]

	260 K	270 K	280 K	290 K	300 K	310 K	suggested value at 298 K[2]
			DMS				
BH&HLYP	1.55×10^{-12}	1.31×10^{-12}	1.13×10^{-12}	9.87×10^{-13}	8.71×10^{-13}	7.77×10^{-13}	1.0×10^{-12}
CCSD(T)	6.90×10^{-12}	5.37×10^{-12}	4.26×10^{-12}	3.45×10^{-13}	2.85×10^{-13}	2.38×10^{-13}	
ref 4	9.04×10^{-13}	8.82×10^{-13}	8.63×10^{-13}	8.45×10^{-13}	8.28×10^{-13}	8.13×10^{-13}	-
ref 7	1.37×10^{-12}	1.27×10^{-12}	1.89×10^{-12}	1.11×10^{-12}	1.05×10^{-12}	9.89×10^{-13}	-
			Methyl Mercaptan				
BH&HLYP	1.50×10^{-9}	9.58×10^{-10}	6.49×10^{-10}	4.53×10^{-10}	3.24×10^{-10}	3.28×10^{-10}	0.9×10^{-12}
CCSD(T)	4.96×10^{-9}	3.01×10^{-9}	1.90×10^{-9}	1.24×10^{-9}	8.36×10^{-10}	5.79×10^{-10}	
ref 4	1.01×10^{-12}	9.23×10^{-13}	8.52×10^{-13}	7.92×10^{-13}	7.39×10^{-13}	6.93×10^{-13}	
			Dimethyl Disulfide				
BH&HLYP (oxygen addition)	1.82×10^{-31}	7.49×10^{-31}	2.81×10^{-30}	9.64×10^{-30}	3.06×10^{-29}	9.06×10^{-29}	
BH&HLYP (hydrogen abstraction)	9.57×10^{-17}	1.23×10^{-16}	1.56×10^{-16}	1.95×10^{-16}	2.40×10^{-16}	2.94×10^{-16}	4.0×10^{-14}
CCSD(T) (hydrogen abstraction)	6.05×10^{-16}	7.08×10^{-16}	8.22×10^{-16}	9.48×10^{-16}	1.09×10^{-15}	1.24×10^{-15}	
BH&HLYP (oxygen addition)[b]	8.75×10^{-31}	3.15×10^{-30}	1.05×10^{-29}	3.27×10^{-29}	9.54×10^{-29}	2.62×10^{-28}	
BH&HLYP (hydrogen abstraction)[b]	1.32×10^{-16}	1.67×10^{-16}	2.09×10^{-16}	2.57×10^{-16}	3.14×10^{-16}	3.80×10^{-16}	4.0×10^{-14}
CCSD(T) (hydrogen abstraction)[b]	8.29×10^{-16}	9.56×10^{-16}	1.10×10^{-15}	1.25×10^{-15}	1.41×10^{-15}	1.59×10^{-15}	
ref 4	5.79×10^{-13}	5.56×10^{-13}	5.35×10^{-13}	5.16×10^{-13}	5.00×10^{-13}	4.84×10^{-13}	

[a] Experimental values are also shown to compare temperature dependence and speed of the rate constant. [b] Because these reactions have positive activation energy, Eckhart tunneling was applied to the rate constant calculations.

attraction of nitrate and DMS is significant because it also explains some obscurities regarding the temperature dependence of the reaction. For example, Tyndall and Ravishankara[2] used the adduct complex to partly explain the negative temperature dependence of reactions 1 and 2. In the atmosphere, a strong reactant complex could be significant because of its high stability, especially at low temperatures.

As both reactions proceed, the interaction between the S and O atoms in the reactant complex gradually disengages until reaction products are fully formed. Simultaneously, the hydrogen atom to be abstracted moves away from the organic sulfide until it is attached to the nitrate radical, forming nitric acid. The optimized geometries at each equilibrium position on the reaction pathway for reaction 1 from the different methods, MP2, B3LYP, BH&HLYP, and BB1K, are similar and consistent, supporting a common reaction pathway. Selected geometrical parameters at the stationary points from MP2/aug-cc-pVDZ and BH&HLYP/6-311++G(d,p) calculations are shown in Figure 2. Furthermore, the calculations on the hydrogen abstraction reaction do not show significant dependence on the basis set, especially with regard to geometries and relative electronic energies.

For reaction 1, the activation energy of about −1 kcal/mol may be suggested from the BH&HLYP and CCSD(T) calcula-

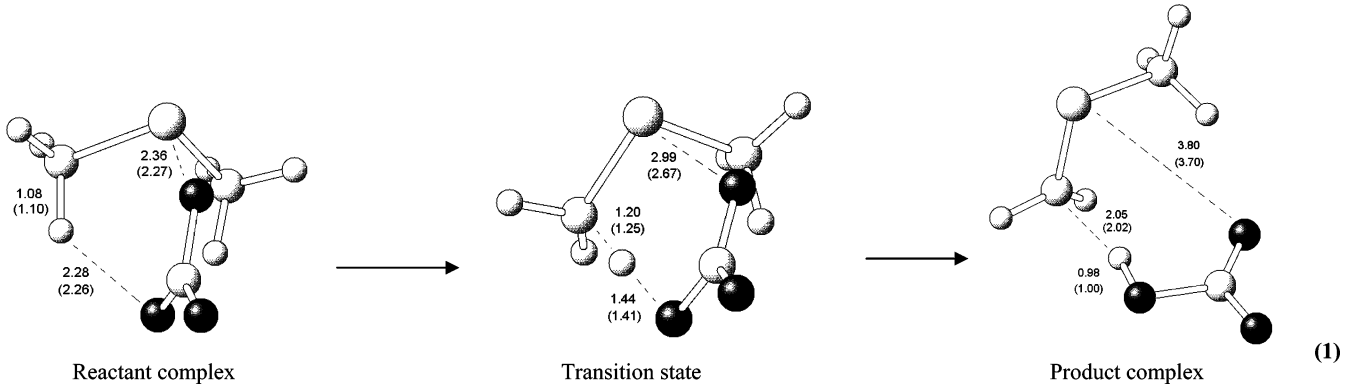

Figure 2. Geometries of reaction 1 with bond distances reported in Å. All geometries were optimized at the BH&HLYP/6-311++G(d,p) level (MP2/aug-cc-pVDZ geometries are shown in parentheses).

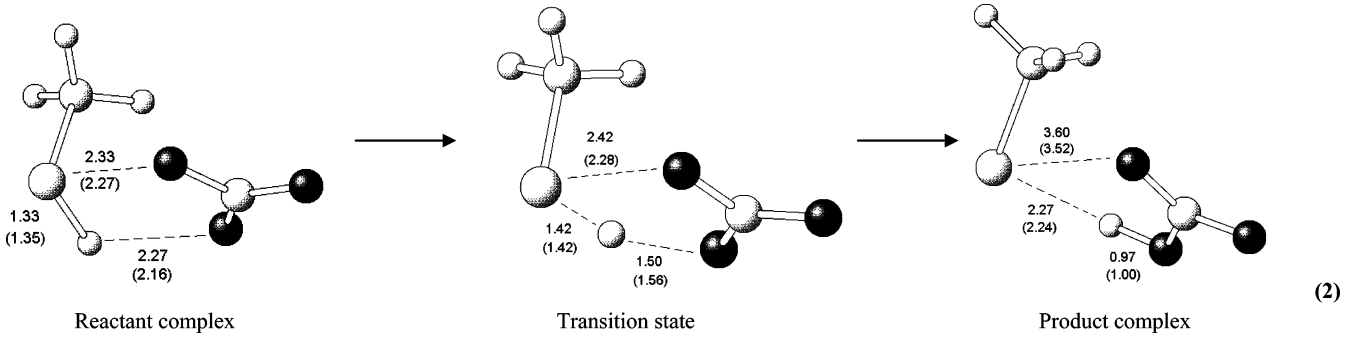

Figure 3. Geometries of reaction 2 with bond distances reported in Å. All geometries were optimized at the BH&HLYP/6-311++G(d,p) level (MP2/aug-cc-pVDZ geometries are shown in parentheses).

tions. B3LYP underestimates the activation energy by about 3 kcal/mol and MP2 overestimates by over 10 kcal/mol as compared to CCSD(T), the highest level of theory. This assessment is consistent with the kinetics calculations. The resulting rate constants are either too high for B3LYP or too low for MP2. Various experiments[2−4] suggest the rate constant for the DMS + NO_3 reaction to be about 1.0×10^{-12} cm^3 $molecule^{-1}$ s^{-1} at 298 K. The rate constant at 300 K derived from B3LYP calculations is 2 orders of magnitude too high, and one from MP2 calculations is 6 orders of magnitude too low. The BB1K theory predicts activation energy even lower than B3LYP, and the corresponding rate constants is 2−3 orders of magnitude too high. The BH&HLYP activation energy appears more reasonable, and the corresponding rate constant at 300 K, 0.87×10^{-13} cm^3 $molecule^{-1}$ s^{-1}, is within 20% of the experimental value. The good result of the BH&HLYP method is in accordance with other computational studies.[20,21] For this reason, the energy diagram in Figure 2 is taken from BH&HLYP calculations. When single point CCSD(T) calculations are performed on the MP2/aug-cc-pVDZ geometries, the relative energies agree closely with those of BH&HLYP. The CCSD(T) activation energy is −0.13 kcal mol^{-1} and the resulting rate constant is 2.85×10^{-12} cm^3 $molecule^{-1}$ s^{-1}, within 30% of the experimental value.

The temperature dependence of the rate constant of the DMS + NO_3• reaction is somewhat controversial. Experimental studies by Atkinson et al.[3] that treated the reaction as first-order, dependent only on the concentration of nitrate, found no dependence on temperature. However, the article by Dlugokencky and Howard[7] predicts a negative temperature dependence for the reaction rate constant, given by the expression $k(T) = 1.79 \times 10^{-13}e^{530/T}$ cm^3 $molecule^{-1}$ s^{-1}. The negative temperature dependence was confirmed by the study by Wallington et al.,[4] who predicted a rate constant given by $k(T) = 4.7 \times 10^{-13}e^{170/T}$ cm^3 $molecule^{-1}$ s^{-1}. This study supports the negative temperature dependence of the rate constant because of the negative activation energy predicted by the most accurate levels of theory (see Table 2). Tyndall and Ravishankara[2] attributed the negative temperature dependence partly to the fact that the reactant complex of pathway 1 is so strong. Unfortunately, classical transition state theory makes it impossible to test this hypothesis through calculation; however, the strength of the reactant complex indicates that this is a possibility.

Other reaction pathways involving nitrate and DMS, including the possibility of addition of oxygen to the sulfur atom producing nitrite and oxygenated sulfur radicals, are declared improbable in experiments because no nitrite is detected in chamber studies.[2−5,7] In agreement with these experimental studies, preliminary B3LYP results predict a high activation energy of at least 10 kcal/mol for such reaction pathways; hence the possibility of oxygen addition to DMS is not considered further.

Methyl Mercaptan. The reaction of methyl mercaptan with nitrate radical proceeds similarly to the previously mentioned reaction of DMS with nitrate radical. As in the case of DMS, the reactant complex of methyl mercaptan with NO_3 appears significant, with bond strength greater than or equal to 10 kcal/mol according to B3LYP and BH&HLYP. Furthermore, the bond distance of the oxygen atom on the nitrate radical and methyl mercaptan's sulfur atom is 2.27 Å, the same as the corresponding bond distance on the DMS reaction. As the reaction proceeds, this bond dissociates until products are formed (see Figure 3).

For the reaction of methyl mercaptan, B3LYP and BH&HLYP calculations consistently predict an activation energy of about −7 kcal mol^{-1}, and CCSD(T) calculations give an activation energy of −5.73 kcal/mol (see Table 1). The corresponding rate constants are about 1−2 orders of magnitude higher than the value suggested by Dlugokencky and Howard[7] of 0.9×10^{-12}

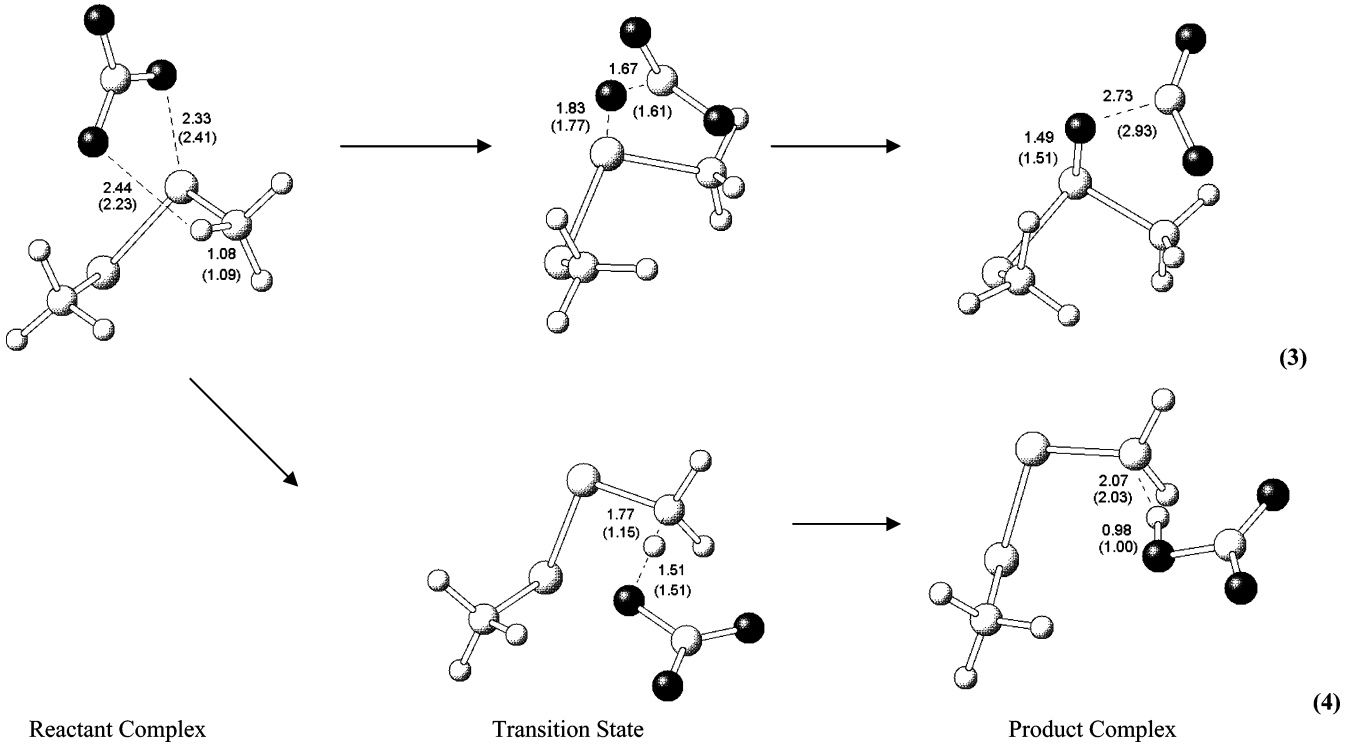

Figure 4. Geometries of reactions 3 and 4 with bond distances reported in Å. All geometries were optimized at the BH&HLYP/6-311++G(d,p) level(MP2/6-31+G(d) geometries are shown in parentheses).

cm^3 $molecule^{-1}$ s^{-1} and the value compiled by Tyndall and Ravishankara[2] of 0.9×10^{-12} cm^3 $molecule^{-1}$ s^{-1} at 298 K. On the other hand, MP2 calculations again predict an energy barrier that is too high, about 3.8 kcal mol^{-1} using the 6-311++G(d,p) basis set and 1.4 kcal mol^{-1} using the aug-cc-pVDZ basis set. The corresponding rate constant is about 2 orders of magnitude too low as compared to the experimental value. On the basis of this analysis, an activation energy of about -4 kcal mol^{-1} is anticipated for the reaction and is within 2 kcal/mol from CCSD(T) calculations.

The negative activation energies reaction from CCSD(T) and BH&HLYP calculations suggest a negative temperature dependence for the rate constants. This implies that the reactions proceed more quickly at lower temperatures and occur at nighttime. This is consistent with the claim by Tyndall and Ravishankara that oxidation of sulfur species by nitrate in general exhibit negative temperature dependence.[2] However, although Dlugokencky and Howard[7] reported negative temperature dependence for reaction 1 between DMS and NO_3, the study reported no dependence on temperature for reaction 2. On the other hand, Wallington et al.[4] predicted a rate constant of $k(T) = 1.0 \times 0^{-13}e^{600/T}$ cm^3 $molecule^{-1}$ s^{-1} implying negative temperature dependence. As in the case of reaction 1, this study supports negative temperature dependence for the methyl mercaptan reaction.

One possible reason for the discrepancy between experiment and theory of the speed of the reaction is the fact that classical transition state theory tends to overestimate rate constants. This is due to the fact that the "width" of the activation energy is not accounted for by the tunneling factors nor by the transition state theory itself. Transition state theory also does not account for recrossing in which the hydrogen atom moves backward and forward along the reaction pathway. Furthermore, other points on the reaction pathway, such as the reactant complex and product complex, are not accounted for in the kinetics calculations. Because the reactant complex has relatively high bond strength in this reaction, one should keep in mind that the kinetics calculations produced for this reaction most likely produce an overestimate of the actual reaction rate constant.

Other reaction pathways involving nitrate methyl mercaptan, including the possibility of addition of oxygen to the sulfur atom producing nitrite and oxygenated sulfur radicals and abstraction from the methyl group rather than the hydrogenated sulfur atom, are declared improbable in experiments because little or no nitrite is detected in experimental studies.[2,7] As in the case of reaction 1, preliminary B3LYP results predict high activation energy of at least 10 kcal mol^{-1} for such reaction pathways; hence the possibility of oxygen addition to methyl mercaptan is also not considered further.

In summary, the results of calculation on the reactions of DMS and methyl mercaptan, reactions 1 and 2, respectively, are in general agreement with available experimental results. The different theories and basis sets have all converged on a common reaction pathway.

Dimethyl Disulfide. The fact that spectral signs of a DMDS–NO_3 adduct complex were not detected in significant quantities by Jensen et al.[12] is explained by the fact that the reactant complex of the DMDS reaction has slightly less dissociation energy than that of DMS according to all levels of theory. Furthermore, when the geometries of the transition state and product complexes of reaction 4 are compared to that of the reactant complex, there appears to be a large change (see Figure 4). When nitrate abstracts from a methyl group, there is no interaction between the sulfur and oxygen atoms; instead, the nitrate molecule moves toward the methyl group so that the electronegative oxygen is attracted to the hydrogen atoms. The distance from one the sulfur atom to the nearest oxygen in this case is 3.49 Å, a large distance compared to the length of the same bond, 2.33 Å, for the reactant complex. This configuration is maintained as one of the hydrogen atoms is transferred to nitrate. Such a geometry would explain why a peroxynitrate compound is only briefly detected using experimental methods.

In fact, a reactant complex may not even be necessary for hydrogen abstraction to occur, because in such a case nitrate could presumably enter a transition state without forming an S−O complex. This hypothesis is further supported by our IRC calculations. According to IRC calculations, the reaction for hydrogen abstraction begins closer to the methyl group than is predicted by reactant complex geometry optimizations; the distance between the oxygen atom on the nitrate radical and the sulfur atom on DMDS is about 1 Å longer than the distance between the oxygen atom on the nitrate radical and the hydrogen atom to be abstracted, so that the geometry more closely resembles that of the transition state of reaction 4.

The first pathway considered for oxidation of DMDS was addition of an oxygen atom to one of the sulfur atoms (3). Considering only reactants and products, this would seem a highly probable reaction pathway. First, the reaction is highly exothermic, even more so than either reaction 1 or 2 ($\Delta E = -18.25$ kcal mol^{-1}); thus products are favored over reactants. Second, when the product complex is formed, we see that the S−S bond length of CH_3SSOCH_3 radical increases by almost 1 Å when compared to the S−S bond length of DMDS. This increasing bond length would indicate the probable formation of CH_3S and CH_3SO radicals, an important step according to the decomposition pathway in Figure 1. However, the possibility of oxygen addition to the sulfur atom is refuted by the fact that it has relatively high activation energy. B3LYP and BB1K predict an energy barrier of at least 10 kcal mol^{-1}, corresponding to a rate constant ranging from more than 10^6 to 10^{16} times slower than the expected value of 0.4×10^{-13} cm^3 molecule^{-1} s^{-1}. BH&HLYP, MP2, and CCSD(T) calculations only predict a higher barrier for the reaction and thus an even slower rate constant. After Eckart tunneling corrections are applied to kinetics calculations at the CCSD(T) and BH&HLYP levels of theory, the result is a rate constant that is still 18 orders of magnitude too slow. After multiple failed attempts to find a different transition state, it becomes clear that oxygen addition to the sulfur atom is highly improbable.

The next considered pathway is hydrogen abstraction from one of the methyl groups forming nitric acid and the CH_3SSCH_2 radical (4). When B3LYP calculations are performed to achieve a transition state for such a reaction, the corresponding activation energy is −2 kcal mol^{-1}. The rate constant obtained from such a pathway is 1.1×10^{-13} to 1.0×10^{-13} cm^3 molecule^{-1} s^{-1} in the range 260−310 K, in excellent agreement with experimentally suggested values.[2,4,7] Furthermore, although BH&HLYP predicts slight positive activation energy and thus a rate constant that is too slow (2.1×10^{-16} cm^3 molecule^{-1} s^{-1} at 300 K), the rate constant for reaction 3 using similar theory is much slower (9.5×10^{-29} cm^3 molecule^{-1} s^{-1}). The same correlation holds true for MP2, BB1K, and extrapolated CCSD(T) values. In fact, when CCSD(T) energy calculations are applied to the BH&HLYP kinetics calculations, the rate constant goes up by about 1 order of magnitude, putting it in better agreement with the value of 4.0×10^{-14} cm^3 molecule^{-1} s^{-1} proposed by Tyndall and Ravishankara.[2] The temperature dependence of this reaction is uncertain according to Dlugokencky and Howard;[7] however, Wallington et al.[4] proposed very slight negative temperature dependence according to the Arrhenius equation $1.9 \times 10^{-13}e^{290/T}$ cm^3 molecule^{-1} s^{-1}. Although the energy calculations according to BH&HLYP and CCSD(T) calculations predict positive activation energy and thus positive temperature dependence for this reaction, the correlation is relatively small. Thus, according to kinetics calculations, it would appear that hydrogen abstraction is by far the much more likely oxidizing mechanism when nitrate interacts with DMDS.

Although this pathway does not fit well with the oxidation mechanism proposed by Jensen et al.,[12] Tyndall and Ravishankara[2] pointed out that the observation of peroxy sulfinyl nitrate does not necessitate a C−S scission and that hydrogen abstraction could also produce CH_3S. The decomposition of the CH_3SSCH_2 radical can be used to explain several questions regarding the percent yield of various products found in experimental scans. The surprisingly high yield of formaldehyde in experiments can be roughly explained by a reaction with NO_X and O_2 producing CH_2O, CH_3S, and SO_2. If DMDS decomposed beginning with hydrogen abstraction, it would have to go through several branching steps before CH_2O could finally form, whereas an immediate reaction between O_2, NO_X, and CH_3SSCH_2 would seem more favorable to the production of CH_2O. This is in fact supported by the fact that NO_X was found necessary for the full decomposition of DMDS in experiments.[12] An even more important issue regarding the branching pattern of CH_3SSCH_2 involves the fate of the extra sulfur atom left after CH_2O is produced. It is clear that most of the sulfur from other reduced sulfur compounds becomes either SO_2 or MSA. The same holds true for DMDS. According to the decomposition diagram by Jensen et al.,[12] the amount of SO_2 and MSA produced from DMS and methyl mercaptan decomposition should be distributed such that about 50% of the sulfur becomes MSA and 17% becomes SO_2. Because DMDS has two sulfur atoms, we would expect the yield of both MSA and SO_2 to increase; however, this is not the case. Though the percent yield of MSA remains around 50%, the amount of SO_2 doubles to about 35%.[12] Thus it would appear that the lingering sulfur atom on the CH_3SS radical reacts with O_2 to form sulfur dioxide. The lingering sulfur atom has important implications because sulfur dioxide eventually transforms into sulfate aerosols and sulfuric acid.[9] According to this decomposition route and data from chamber experiments, each molecule of DMDS produces twice as much sulfur dioxide as a molecule of DMS or methyl mercaptan.

A problem with some experimental work involving the decomposition of DMDS is that it is sometimes regenerated shortly after it reacts with nitrate.[2] Although this could be due to a reverse reaction between nitric acid and CH_3SSCH_2, work done in this study shows that this is not the case. Although reaction 4 is the least exothermic of the reactions considered, its Gibbs free energy value ($\Delta G = -9.28$ kcal mol^{-1}) is negative enough that the reaction proceeds in a direction overwhelmingly favoring the products over reactants. Equilibrium constants derived from kinetics calculations on these ΔG values imply that the reaction is not highly reversible. Thus the regeneration of DMDS is likely due to recombination of CH_3S radicals rather than a reversal of the original oxidation reaction. This recombination indicates that the formation of nitric acid via reaction with DMDS could lead to a major sink for nitrate radical in the atmosphere, as DMDS could be regenerated in great quantity even after it completes its initial reaction with nitrate.

Conclusion

Several inferences regarding the reaction between nitrate and reduced sulfur compounds can be made on the basis of theoretical calculations. The oxygen addition to the sulfur atom as described by eq 3 is unlikely due to a rather high activation energy for such a pathway. As a result, the reactions of nitrate radical with all three organic sulfides follow the hydrogen abstraction pathways. The initial adduct of each reaction is

significant as it represents a strong attraction between the reacting nitrate and sulfur in the troposphere. Kinetics calculations predict relatively fast rate constants for abstraction reactions (1) and (2), and a moderately slow speed for reaction (4). Considering the sensitivity of these calculations to different levels of theory, the predictions for reactions 1 and 4 are in good agreement with experimental values whereas the overestimation of the rate constant in the case of reaction 2 can probably be accounted for by the previously mentioned problems with transition state theory.

The study may have significant atmospheric implications. Because of the relatively large rate constants predicted for reactions (1) and (2), the reactions of methyl mercaptan and DMS with nitrate radical are of great importance in the atmosphere; however, because the concentration of DMDS is lower than that of DMS in the atmosphere and the rate constant for the DMDS + NO_3 radical is relatively slow, the reaction may not be as important in the atmosphere. Nonetheless, the idea that nitrate can serve as a sink for reduced sulfur compounds and vice versa is certainly validated in the case of DMS, methyl mercaptan, and DMDS, in agreement with field studies.[25,26] The study also shows nitrate reactions with organic sulfides have, for the most part, negative activation energy and thus negative temperature dependence. The fact that the nitrate−sulfur reactions considered in this study occur more rapidly at colder temperatures validates the nighttime occurrence of these reactions.

Acknowledgment. This work was supported in part by The Camille and Henry Dreyfus Foundation (Award No. TH-00-028) and California State University, Fullerton. We also thank Professor Thanh N. Truong of University of Utah for the use of their online service in the kinetics theory.

References and Notes

(1) Bates, T. S.; Lamb, B. K.; Guenther, A.; Dignon, J.; Stoiber, R. E. *J. Atmos. Chem.* **1992**, *14*, 315.

(2) Tyndall, G. S.; Ravishankara, A. R. *Int. J. Chem. Kinetics* **1991**, *23*, 483.

(3) Atkinson, R.; Pitts, J. N.; Aschmann, S. M. *J. Phys. Chem.* **1984**, *88*, 1584.

(4) Wallington, T. J.; Atkinson, R.; Winer, A. M.; Pitts, J. N. *J. Phys. Chem.* **1986**, *90*, 5393.

(5) Jensen, N. R.; Hjorth, J.; Lohse, C.; Skov, H.; Restelli, G. *Atmos. Environ.* **1991**, *25A*, 1897.

(6) Tyndall, G. S.; Burrows, J. P.; Schneider, W.; Moortgat, G. K. *Chem Phys Lett*. **1986**, *92*, 91, 1988.

(7) Dlugokencky, E. J.; Howard, C. J. *J. Phys. Chem*. **1988**, *92*, 1188.

(8) Winer, A. M.; Atkinson, R.; Pitts, J. N., Jr. *Science* **1984**, *224*, 156.

(9) Toole, D. A.; Kieber, D. J.; Kiene, R. P.; White, E. M.; Bisgrove, J.; del Valle, D. A.; Slezak, D. *Geophys. Res. Lett.* **2004**, *31*, L11307.

(10) Bardouki, H.; Berresheim, H.; Vrekoussis, M.; Sciare, J.; Kouvarakis, G.; Oikonomou, L. K.; Schneider, J.; Mihalopoulos, N. *Atmos. Chem. Phys. Discuss*. **2003**, *3*, 3869.

(11) Seinfeld, J. H.; Pandis, S. N. *Atmospheric Chemistry and Physics: From Air Pollution to Climate Change*; John Wiley and Sons: New York, 1998.

(12) Jensen, N. R.; Hjorth, J.; Lohse, C.; Skov H.; Restelli, G. *J. Atmos. Chem*. **1992**, *14*, 95.

(13) Daykin, E. P.; Wine, P. H. *Int. J. Chem. Kinet.* **1990**, *22*, 1083.

(14) Jefferson, A.; Tanner, D. J.; Eisele, F. L.; Berresheim, H. *J. Geophys. Res*. **1998**, *103*, 1639.

(15) MacLeod, H.; Aschmann, S. M.; Atkinson, R.; Tuazon, E. C.; Sweetman, J. A. *J. Geophys. Res.* **1986**, *91*, 5338.

(16) Frisch, M. J.; Trucks, G. W.; Schlegel, H. B.; Scuseria, G. E.; Robb, M. A.; Cheeseman, J. R.; Montgomery, J. A., Jr.; Vreven, T.; Kudin, K. N.; Burant, J. C.; Millam, J. M.; Iyengar, S. S.; Tomasi, J.; Barone, V.; Mennucci, B.; Cossi, M.; Scalmani, G.; Rega, N.; Petersson, G. A.; Nakatsuji, H.; Hada, M.; Ehara, M.; Toyota, K.; Fukuda, R.; Hasegawa, J.; Ishida, M.; Nakajima, T.; Honda, Y.; Kitao, O.; Nakai, H.; Klene, M.; Li, X.; Knox, J. E.; Hratchian, H. P.; Cross, J. B.; Adamo, C.; Jaramillo, J.; Gomperts, R.; Stratmann, R. E.; Yazyev, O.; Austin, A. J.; Cammi, R.; Pomelli, C.; Ochterski, J. W.; Ayala, P. Y.; Morokuma, K.; Voth, G. A.; Salvador, P.; Dannenberg, J. J.; Zakrzewski, V. G.; Dapprich, S.; Daniels, A. D.; Strain, M. C.; Farkas, O.; Malick, D. K.; Rabuck, A. D.; Raghavachari, K.; Foresman, J. B.; Ortiz, J. V.; Cui, Q.; Baboul, A. G.; Clifford, S.; Cioslowski, J.; Stefanov, B. B.; Liu, G.; Liashenko, A.; Piskorz, P.; Komaromi, I.; Martin, R. L.; Fox, D. J.; Keith, T.; Al-Laham, M. A.; Peng, C. Y.; Nanayakkara, A.; Challacombe, M.; Gill, P. M. W.; Johnson, B.; Chen, W.; Wong, M. W.; Gonzalez, C.; Pople, J. A. *Gaussian 03*, revision C.01; Gaussian, Inc., Wallingford, CT, 2004.

(17) Janoschek, R. *Pure Appl. Chem.* **2001**, *73*, 9, 1521.

(18) Becke, A. D. *J. Phys Chem*. **1993**, *98*, 1372.

(19) Zhao, Y.; Lynch, B. J.; Truhlar, D. G. *J. Phys. Chem.* **2004**, *108*, 2715.

(20) Gonzales-Garcia, N.; Gonzales-Lafont, À.; Lluch, J. M. *J. Comput. Chem*. **2005**, *26*, 569.

(21) Li, Q. S.; Wang, C. Y. *J. Phys Chem*. **2002**, *106*, 8883.

(22) Wolinski, K.; Pulay, P. *J. Chem. Phys.* **1989**, *90*, 7, 3647.

(23) Raghavachari, K.; Trucks, G. W.; Pople, J. A.; Head-Gordon, M. *Chem. Phys. Lett.* **1989**, *157*, 479.

(24) Zhang, S.; Truong, T. N. *Kinetics*; CSEO Version 1.0; University of Utah, 2001.

(25) Allan, B. J.; Carslaw, N.; Coe, H.; Burgess, R. A.; Plane, J. M. C. *J. Atmos. Chem*. **1999**, *33*, 129.

(26) Vrekoussis, M.; Kanakidou, M.; Mihalopoulos, N.; Crutzen, P. J.; Lelieveld, J.; Perner, D.; Berresheim, H.; Baboukas, E. *Atmos. Chem. Phys. Discuss*. **2003**, *3*, 3135−3196.